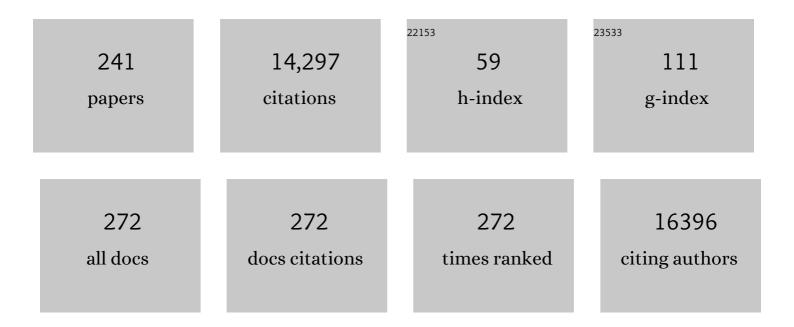
Junliang Sun

List of Publications by Year in descending order

Source: https://exaly.com/author-pdf/9131776/publications.pdf Version: 2024-02-01



LUNUANC SUN

#	Article	IF	CITATIONS
1	Tailoring the Pore Surface of 3D Covalent Organic Frameworks via Postâ€&ynthetic Click Chemistry. Angewandte Chemie, 2022, 134, .	2.0	11
2	Tailoring the Pore Surface of 3D Covalent Organic Frameworks via Postâ€Synthetic Click Chemistry. Angewandte Chemie - International Edition, 2022, 61, .	13.8	44
3	SCM-25: A Zeolite with Ordered Meso-cavities Interconnected by 12Â×Â12Â×Â10-Ring Channels Determined b 3D Electron Diffraction. Inorganic Chemistry, 2022, 61, 4371-4377.	ру 4.0	5
4	A general method for searching for homometric structures. Acta Crystallographica Section B: Structural Science, Crystal Engineering and Materials, 2022, 78, 14-19.	1.1	1
5	Crystal structure and optical performance analysis of a new type of persistent luminescence material with multi-functional application prospects. Journal of Energy Chemistry, 2022, 69, 150-160.	12.9	9
6	Synthesis of crystalline WS ₃ with a layered structure and desert-rose-like morphology. Nanoscale Advances, 2022, 4, 1626-1631.	4.6	2
7	Accurate structure determination of nanocrystals by continuous precession electron diffraction tomography. Science China Materials, 2022, 65, 1417-1420.	6.3	3
8	Design and Synthesis of a Zeolitic Organic Framework**. Angewandte Chemie - International Edition, 2022, 61, .	13.8	14
9	Achieving ultrahigh electrochemical performance by surface design and nanoconfined water manipulation. National Science Review, 2022, 9, .	9.5	9
10	Synthesis, Structure and Superconducting Properties of Ba1-xLax/4K3x/4(Bi0.25Pb0.75)O3- Perovskites. Physica C: Superconductivity and Its Applications, 2022, 598, 1354075.	1.2	0
11	Borates as a new direction in the design of oxide ion conductors. Science China Materials, 2022, 65, 2737-2745.	6.3	8
12	Atomic-resolution structures from polycrystalline covalent organic frameworks with enhanced cryo-cRED. Nature Communications, 2022, 13, .	12.8	10
13	HPMâ€14: A New Germanosilicate Zeolite with Interconnected Extraâ€Large Pores Plus Oddâ€Membered and Small Pores**. Angewandte Chemie - International Edition, 2021, 60, 3438-3442.	13.8	15
14	Atomically precise single-crystal structures of electrically conducting 2D metal–organic frameworks. Nature Materials, 2021, 20, 222-228.	27.5	239
15	Triptycene-based three-dimensional covalent organic frameworks with stp topology of honeycomb structure. Materials Chemistry Frontiers, 2021, 5, 944-949.	5.9	26
16	Structure–direction towards the new large pore zeolite NUD-3. Chemical Communications, 2021, 57, 191-194.	4.1	15
17	HPMâ€14: A New Germanosilicate Zeolite with Interconnected Extraâ€Large Pores Plus Oddâ€Membered and Small Pores**. Angewandte Chemie, 2021, 133, 3480-3484.	2.0	5
18	Rare earth elements based oxide ion conductors. Inorganic Chemistry Frontiers, 2021, 8, 1374-1398.	6.0	24

#	Article	IF	CITATIONS
19	Binding and separation of CO ₂ , SO ₂ and C ₂ H ₂ in homo- and hetero-metallic metal–organic framework materials. Journal of Materials Chemistry A, 2021, 9, 7190-7197.	10.3	17
20	A Crystalline Three-Dimensional Covalent Organic Framework with Flexible Building Blocks. Journal of the American Chemical Society, 2021, 143, 2123-2129.	13.7	105
21	Guest-Binding-Induced Interhetero Hosts Charge Transfer Crystallization: Selective Coloration of Commonly Used Organic Solvents. Journal of the American Chemical Society, 2021, 143, 1553-1561.	13.7	38
22	An Intriguing Polarization Configuration of Mixed Ising- and Néel-Type Model in the Prototype PbZrO ₃ -Based Antiferroelectrics. Inorganic Chemistry, 2021, 60, 3232-3237.	4.0	8
23	Structural origin of the high-voltage instability of lithium cobalt oxide. Nature Nanotechnology, 2021, 16, 599-605.	31.5	148
24	A Deepâ€UV Nonlinear Optical Borosulfate with Incommensurate Modulations. Angewandte Chemie, 2021, 133, 11558-11564.	2.0	11
25	A Deepâ€UV Nonlinear Optical Borosulfate with Incommensurate Modulations. Angewandte Chemie - International Edition, 2021, 60, 11457-11463.	13.8	37
26	Stable, Efficient, Copper Coordination Polymer-Derived Heterostructured Catalyst for Oxygen Evolution under pH-Universal Conditions. ACS Applied Materials & Interfaces, 2021, 13, 25461-25471.	8.0	7
27	EMM-25: The Structure of Two-Dimensional 11 × 10 Medium-Pore Borosilicate Zeolite Unraveled Using 3D Electron Diffraction. Chemistry of Materials, 2021, 33, 4146-4153.	6.7	11
28	Tuning the Topology of Three-Dimensional Covalent Organic Frameworks via Steric Control: From pts to Unprecedented ljh . Journal of the American Chemical Society, 2021, 143, 7279-7284.	13.7	84
29	Guest-Induced Switching of a Molecule-Based Magnet in a 3d–4f Heterometallic Cluster-Based Chain Structure. Inorganic Chemistry, 2021, 60, 633-641.	4.0	6
30	Crystalline Sponge Method by Three-Dimensional Electron Diffraction. Frontiers in Molecular Biosciences, 2021, 8, 821927.	3.5	3
31	Constructing Concentration and Temperature Controllable Blue-Green Emission in a Single-Component Solid-State Phosphor. Journal of Physical Chemistry C, 2021, 125, 27420-27428.	3.1	1
32	3D Electron Diffraction Unravels the New Zeolite ECNUâ€23 from the "Pure―Powder Sample of ECNUâ€21. Angewandte Chemie, 2020, 132, 1182-1186.	2.0	8
33	3D Electron Diffraction Unravels the New Zeolite ECNUâ€23 from the "Pure―Powder Sample of ECNUâ€21. Angewandte Chemie - International Edition, 2020, 59, 1166-1170.	13.8	27
34	Synthesis and characterizations of TiN–SBA-15 mesoporous materials for CO ₂ dry reforming enhancement. Pure and Applied Chemistry, 2020, 92, 545-556.	1.9	2
35	Nonmetallic metal toward a pressure-induced bad-metal state in two-dimensional Cu ₃ LiRu ₂ O ₆ . Chemical Communications, 2020, 56, 265-268.	4.1	5
36	Atomically Dispersed Mo Supported on Metallic Co ₉ S ₈ Nanoflakes as an Advanced Nobleâ€Metalâ€Free Bifunctional Water Splitting Catalyst Working in Universal pH Conditions. Advanced Energy Materials, 2020, 10, 1903137.	19.5	162

#	Article	IF	CITATIONS
37	2D and 3D Porphyrinic Covalent Organic Frameworks: The Influence of Dimensionality on Functionality. Angewandte Chemie - International Edition, 2020, 59, 3624-3629.	13.8	227
38	2D and 3D Porphyrinic Covalent Organic Frameworks: The Influence of Dimensionality on Functionality. Angewandte Chemie, 2020, 132, 3653-3658.	2.0	45
39	Highly Conducting Organic–Inorganic Hybrid Copper Sulfides Cu x C 6 S 6 (x=4 or 5.5): Ligandâ€Based Oxidationâ€Induced Chemical and Electronic Structure Modulation. Angewandte Chemie, 2020, 132, 22791-22798.	2.0	2
40	Redox-triggered switching in three-dimensional covalent organic frameworks. Nature Communications, 2020, 11, 4919.	12.8	49
41	Acetonitrileâ€Based Electrolytes for Rechargeable Zinc Batteries. Energy Technology, 2020, 8, 2000358.	3.8	19
42	Diverse crystal size effects in covalent organic frameworks. Nature Communications, 2020, 11, 6128.	12.8	55
43	Paramagnetic Conducting Metal–Organic Frameworks with Threeâ€Dimensional Structure. Angewandte Chemie, 2020, 132, 21059-21064.	2.0	4
44	Synthesis, structure, and superconductivity of B-site doped perovskite bismuth lead oxide with indium. Inorganic Chemistry Frontiers, 2020, 7, 3561-3570.	6.0	14
45	Room Temperature Zero Thermal Expansion in a Cubic Cobaltite. Journal of Physical Chemistry Letters, 2020, 11, 6785-6790.	4.6	6
46	Direct plasma phosphorization of Cu foam for Li ion batteries. Journal of Materials Chemistry A, 2020, 8, 16920-16925.	10.3	44
47	Rational Manipulation of Stacking Arrangements in Threeâ€Dimensional Zeolites Built from Twoâ€Dimensional Zeolitic Nanosheets. Angewandte Chemie, 2020, 132, 20106-20111.	2.0	0
48	Paramagnetic Conducting Metal–Organic Frameworks with Threeâ€Dimensional Structure. Angewandte Chemie - International Edition, 2020, 59, 20873-20878.	13.8	30
49	Adsorption of Nitrogen Dioxide in a Redox-Active Vanadium Metal–Organic Framework Material. Journal of the American Chemical Society, 2020, 142, 15235-15239.	13.7	50
50	Rational Manipulation of Stacking Arrangements in Threeâ€Dimensional Zeolites Built from Twoâ€Dimensional Zeolitic Nanosheets. Angewandte Chemie - International Edition, 2020, 59, 19934-19939.	13.8	4
51	Collective and individual impacts of the cascade doping of alkali cations in perovskite single crystals. Journal of Materials Chemistry C, 2020, 8, 15351-15360.	5.5	1
52	Guest-Controlled Incommensurate Modulation in a Meta-Rigid Metal–Organic Framework Material. Journal of the American Chemical Society, 2020, 142, 19189-19197.	13.7	24
53	Modulated structure determination and ion transport mechanism of oxide-ion conductor CeNbO4+l´. Nature Communications, 2020, 11, 4751.	12.8	20
54	Highly Conducting Organic–Inorganic Hybrid Copper Sulfides Cu _{<i>x</i>} C ₆ S ₆ (x=4 or 5.5): Ligandâ€Based Oxidationâ€Induced Chemical and Electronic Structure Modulation. Angewandte Chemie - International Edition, 2020, 59, 22602-22609.	13.8	26

#	Article	IF	CITATIONS
55	Divergent Chemistry Paths for 3D and 1D Metalloâ€Covalent Organic Frameworks (COFs). Angewandte Chemie, 2020, 132, 11624-11629.	2.0	10
56	IDMâ€1: A Zeolite with Intersecting Medium and Extraâ€Large Pores Built as an Expansion of Zeolite MFI. Angewandte Chemie, 2020, 132, 11379-11382.	2.0	12
57	Seeded growth of large single-crystal copper foils with high-index facets. Nature, 2020, 581, 406-410.	27.8	116
58	Single crystal of a one-dimensional metallo-covalent organic framework. Nature Communications, 2020, 11, 1434.	12.8	77
59	Divergent Chemistry Paths for 3D and 1D Metalloâ€Covalent Organic Frameworks (COFs). Angewandte Chemie - International Edition, 2020, 59, 11527-11532.	13.8	35
60	Processing Natural Wood into an Efficient and Durable Solar Steam Generation Device. ACS Applied Materials & Interfaces, 2020, 12, 18165-18173.	8.0	58
61	Nonâ€Interpenetrated Singleâ€Crystal Covalent Organic Frameworks. Angewandte Chemie - International Edition, 2020, 59, 17991-17995.	13.8	60
62	Nonâ€Interpenetrated Singleâ€Crystal Covalent Organic Frameworks. Angewandte Chemie, 2020, 132, 18147-18151.	2.0	5
63	Twist Building Blocks from Planar to Tetrahedral for the Synthesis of Covalent Organic Frameworks. Journal of the American Chemical Society, 2020, 142, 3718-3723.	13.7	83
64	Quasicrystal-related mosaics with periodic lattices interlaid with aperiodic tiles. Acta Crystallographica Section A: Foundations and Advances, 2020, 76, 137-144.	0.1	3
65	An intriguing intermediate state as a bridge between antiferroelectric and ferroelectric perovskites. Materials Horizons, 2020, 7, 1912-1918.	12.2	34
66	A ₂ SnS ₅ : A Structural Incommensurate Modulation Exhibiting Strong Secondâ€Harmonic Generation and a High Laserâ€Induced Damage Threshold (A=Ba, Sr). Angewandte Chemie - International Edition, 2020, 59, 11861-11865.	13.8	67
67	IDMâ€1: A Zeolite with Intersecting Medium and Extraâ€Large Pores Built as an Expansion of Zeolite MFI. Angewandte Chemie - International Edition, 2020, 59, 11283-11286.	13.8	17
68	A ₂ SnS ₅ : A Structural Incommensurate Modulation Exhibiting Strong Secondâ€Harmonic Generation and a High Laserâ€Induced Damage Threshold (A=Ba, Sr). Angewandte Chemie, 2020, 132, 11959-11963.	2.0	17
69	Rational design of crystalline two-dimensional frameworks with highly complicated topological structures. Nature Communications, 2019, 10, 4609.	12.8	54
70	Flexible Freestanding MoO 3â^' x –Carbon Nanotubes–Nanocellulose Paper Electrodes for Charge‣torage Applications. ChemSusChem, 2019, 12, 5157-5163.	6.8	20
71	Multistep nucleation and growth mechanisms of organic crystals from amorphous solid states. Nature Communications, 2019, 10, 3872.	12.8	57
72	DMAP-Induced Gallium Phosphites with Different Dimensionality. Crystal Growth and Design, 2019, 19, 6011-6016.	3.0	4

#	Article	IF	CITATIONS
73	Maximizing sinusoidal channels of HZSM-5 for high shape-selectivity to p-xylene. Nature Communications, 2019, 10, 4348.	12.8	102
74	Mechanistic Insights into Solid-State p-Type Dye-Sensitized Solar Cells. Journal of Physical Chemistry C, 2019, 123, 26151-26160.	3.1	3
75	Photoinduced synthesis of Bi ₂ O ₃ nanotubes based on oriented attachment. Journal of Materials Chemistry A, 2019, 7, 1424-1428.	10.3	9
76	Hydroxyl free radical route to the stable siliceous Ti-UTL with extra-large pores for oxidative desulfurization. Chemical Communications, 2019, 55, 1390-1393.	4.1	39
77	Insights into the Exfoliation Process of V ₂ O ₅ · <i>n</i> H ₂ O Nanosheet Formation Using Real-Time ⁵¹ V NMR. ACS Omega, 2019, 4, 10899-10905.	3.5	12
78	A heavy metal-free CuInS ₂ quantum dot sensitized NiO photocathode with a Re molecular catalyst for photoelectrochemical CO ₂ reduction. Chemical Communications, 2019, 55, 7918-7921.	4.1	21
79	Isostructural Threeâ€Ðimensional Covalent Organic Frameworks. Angewandte Chemie, 2019, 131, 9872-9877.	2.0	31
80	Isostructural Threeâ€Dimensional Covalent Organic Frameworks. Angewandte Chemie - International Edition, 2019, 58, 9770-9775.	13.8	126
81	A New Layered Silicogermanate PKU-23 and Its Transformation to a Zeolite with Three-Dimensional Channels. Crystal Growth and Design, 2019, 19, 2272-2278.	3.0	2
82	Superconductivity in Perovskite Ba _{1â~`x} K _x Bi _{0.30} Pb _{0.70} O _{3â~´Î~} . ChemistrySelect, 2019, 4, 3135-3139.	1.5	7
83	Discovery of Complex Metal Oxide Materials by Rapid Phase Identification and Structure Determination. Journal of the American Chemical Society, 2019, 141, 4990-4996.	13.7	17
84	An NHC-CuCl functionalized metal–organic framework for catalyzing β-boration of α,β-unsaturated carbonyl compounds. Dalton Transactions, 2019, 48, 5144-5148.	3.3	7
85	Synthesis, characterization and structure of (NH ₄) ₄ [Zn ₅ VIV4VV16O ₅₆ H ₂ (H ₂) with a novel V ₅ O ₁₄ layer. Dalton Transactions, 2019, 48, 4906-4911.	O) 3.s ub>4	<b 읿b>]
86	Loneâ€Pair Enhanced Birefringence in an Alkalineâ€Earth Metal Tin(II) Phosphate BaSn ₂ (PO ₄) ₂ . Chemistry - A European Journal, 2019, 25, 5648-5651.	3.3	95
87	Organic Semiconducting Alloys with Tunable Energy Levels. Journal of the American Chemical Society, 2019, 141, 6561-6568.	13.7	65
88	Cage Based Crystalline Covalent Organic Frameworks. Journal of the American Chemical Society, 2019, 141, 3843-3848.	13.7	84
89	An Interrupted Zeolite PKUâ€26 and Its Transformation to a Fully Fourâ€Connected Zeolite PKUâ€27 upon Calcination. Chemistry - A European Journal, 2019, 25, 3219-3223.	3.3	4
90	Pressure-induced semiconductor-to-metal phase transition of a charge-ordered indium halide perovskite. Proceedings of the National Academy of Sciences of the United States of America, 2019, 116, 23404-23409.	7.1	45

#	Article	IF	CITATIONS
91	Achieving Highly Efficient Catalysts for Hydrogen Evolution Reaction by Electronic State Modification of Platinum on Versatile Ti ₃ C ₂ T _{<i>x</i>} (MXene). ACS Sustainable Chemistry and Engineering, 2019, 7, 4266-4273.	6.7	79
92	Synthesis and Structure Determination of SCMâ€15: A 3D Large Pore Zeolite with Interconnected Straight 12×12×10â€Ring Channels. Chemistry - A European Journal, 2019, 25, 2184-2188.	3.3	25
93	Molybdenum Oxide Nanosheets with Tunable Plasmonic Resonance: Aqueous Exfoliation Synthesis and Charge Storage Applications. Advanced Functional Materials, 2019, 29, 1806699.	14.9	55
94	V2O5·nH2O nanosheets and multi-walled carbon nanotube composite as a negative electrode for sodium-ion batteries. Journal of Energy Chemistry, 2019, 30, 145-151.	12.9	26
95	Superconductivity in Perovskite Ba0.85â^'xLaxPr0.15(Bi0.20Pb0.80)O3â^'δ. Journal of Superconductivity and Novel Magnetism, 2019, 32, 167-173.	1.8	4
96	Elucidation of correlated disorder in zeolite IM-18. Acta Crystallographica Section B: Structural Science, Crystal Engineering and Materials, 2019, 75, 333-342.	1.1	3
97	Facile Water-Based Strategy for Synthesizing MoO _{3–<i>x</i>} Nanosheets: Efficient Visible Light Photocatalysts for Dye Degradation. ACS Omega, 2018, 3, 2193-2201.	3.5	135
98	An Open-Framework Aluminophosphite with Face-Sharing AlO ₆ Octahedra Dimers and Extra-Large 14-Ring Channels. Crystal Growth and Design, 2018, 18, 1267-1271.	3.0	8
99	Thermochromic halide perovskite solar cells. Nature Materials, 2018, 17, 261-267.	27.5	630
100	Superconductivity in Perovskite Ba _{1–<i>x</i>} Ln _{<i>x</i>} (Bi _{0.20} Pb _{0.80})O _{3â^î^} (Ln = La, Ce, Pr, Nd, Sm, Eu, Gd, Tb, Dy, Ho, Er, Tm, Yb, Lu). Inorganic Chemistry, 2018, 57, 1269-1276.	4.0	17
101	Synthesis and crystal structure of Sr ₃ Bi ₂ O ₆ and structural change in the strontium–bismuth-oxide system. Dalton Transactions, 2018, 47, 1888-1894.	3.3	7
102	Highly Diastereo―and Enantioselective Cascade Synthesis of Bicyclic Lactams in Oneâ€Pot. European Journal of Organic Chemistry, 2018, 2018, 1158-1164.	2.4	6
103	Three-Dimensional Open-Framework Germanate Built from a Novel Ge ₁₃ Cluster and Containing Two Types of Chiral Layers. Crystal Growth and Design, 2018, 18, 928-933.	3.0	3
104	Topologically guided tuning of Zr-MOF pore structures for highly selective separation of C6 alkane isomers. Nature Communications, 2018, 9, 1745.	12.8	251
105	CsSiB ₃ O ₇ : A Beryllium-Free Deep-Ultraviolet Nonlinear Optical Material Discovered by the Combination of Electron Diffraction and First-Principles Calculations. Chemistry of Materials, 2018, 30, 2203-2207.	6.7	39
106	Water Oxidation Initiated by In Situ Dimerization of the Molecular Ru(pdc) Catalyst. ACS Catalysis, 2018, 8, 4375-4382.	11.2	25
107	A Facile and Green Method for the Synthesis of SFE Borosilicate Zeolite and Its Heteroatom‣ubstituted Analogues with Promising Catalytic Performances. Chemistry - A European Journal, 2018, 24, 306-311.	3.3	7
108	Diphosphine-induced chiral propeller arrangement of gold nanoclusters for singlet oxygen photogeneration. Nano Research, 2018, 11, 5787-5798.	10.4	53

#	Article	IF	CITATIONS
109	An AlEgen-based 3D covalent organic framework for white light-emitting diodes. Nature Communications, 2018, 9, 5234.	12.8	293
110	Synthesis, Structure, and Properties of the Non-Centrosymmeteric Compound LiNaRbB ₅ O ₈ (OH) ₂ . Crystal Growth and Design, 2018, 18, 5745-5749.	3.0	2
111	Highly Conducting Neutral Coordination Polymer with Infinite Two-Dimensional Silver–Sulfur Networks. Journal of the American Chemical Society, 2018, 140, 15153-15156.	13.7	97
112	Synthesis and Structure of a Layered Fluoroaluminophosphate and Its Transformation to a Three-Dimensional Zeotype Framework. Inorganic Chemistry, 2018, 57, 11753-11760.	4.0	7
113	The Exploration of Carrier Behavior in the Inverted Mixed Perovskite Singleâ€Crystal Solar Cells. Advanced Materials Interfaces, 2018, 5, 1800224.	3.7	58
114	Frontispiece: A Facile and Green Method for the Synthesis of SFE Borosilicate Zeolite and Its Heteroatom‣ubstituted Analogues with Promising Catalytic Performances. Chemistry - A European Journal, 2018, 24, .	3.3	0
115	Observation of Interpenetration Isomerism in Covalent Organic Frameworks. Journal of the American Chemical Society, 2018, 140, 6763-6766.	13.7	144
116	One-pot synthesis of Cu-modified HNb ₃ O ₈ nanobelts with enhanced photocatalytic hydrogen production. Journal of Materials Chemistry A, 2018, 6, 10769-10775.	10.3	7
117	Emergent superconductivity in an iron-based honeycomb lattice initiated by pressure-driven spin-crossover. Nature Communications, 2018, 9, 1914.	12.8	119
118	Single-crystal x-ray diffraction structures of covalent organic frameworks. Science, 2018, 361, 48-52.	12.6	868
119	Crystallization of a Novel Germanosilicate ECNUâ€16 Provides Insights into the Spaceâ€Filling Effect on Zeolite Crystal Symmetry. Chemistry - A European Journal, 2018, 24, 9247-9253.	3.3	11
120	Ba3Mg3(BO3)3F3 polymorphs with reversible phase transition and high performances as ultraviolet nonlinear optical materials. Nature Communications, 2018, 9, 3089.	12.8	314
121	Hierarchical Shellâ€Like ZSMâ€5 with Tunable Porosity Synthesized by using a Dissolution–Recrystallization Approach. Chemistry - A European Journal, 2018, 24, 14974-14981.	3.3	15
122	Covalently linking CuInS ₂ quantum dots with a Re catalyst by click reaction for photocatalytic CO ₂ reduction. Dalton Transactions, 2018, 47, 10775-10783.	3.3	37
123	Effect of zinc doping on structural, magnetic and dielectric properties of perovskite (Tb0.874Mn0.106)MnO3â^î^. Journal of Materials Science: Materials in Electronics, 2018, 29, 16543-16552.	2.2	0
124	Discovery of Layered Indium Hydroxide via a Hydroperoxyl Anion Coordinated Precursor at Room Temperature. Chemistry - A European Journal, 2018, 24, 15491-15494.	3.3	0
125	Reversible adsorption of nitrogen dioxide within a robust porous metal–organic framework. Nature Materials, 2018, 17, 691-696.	27.5	162
126	Synthesis and characterization of germanosilicate molecular sieves: GeO ₂ /SiO ₂ ratio, H ₂ O/TO ₂ ratio and temperature. Dalton Transactions, 2017, 46, 2270-2280.	3.3	13

#	Article	IF	CITATIONS
127	Enhancement of Ferroelectricity for Orthorhombic (Tb _{0.861} Mn _{0.121})MnO _{3â^Î} by Copper Doping. Inorganic Chemistry, 2017, 56, 3475-3482.	4.0	11
128	Achieving High Pseudocapacitance of 2D Titanium Carbide (MXene) by Cation Intercalation and Surface Modification. Advanced Energy Materials, 2017, 7, 1602725.	19.5	514
129	Synthesis, structure and magnetic properties of (Eu1â^xMnx)MnO3â^î^. RSC Advances, 2017, 7, 2019-2024.	3.6	13
130	Electron Crystallography Reveals Atomic Structures of Metal–Organic Nanoplates with M ₁₂ (μ ₃ -O) ₈ (μ ₃ -OH) ₈ (μ _{-OH) (M = Zr, Hf) Secondary Building Units. Inorganic Chemistry, 2017, 56, 8128-8134.}	4)< ≇n p>6∢	(51612>
131	Simple CTAB surfactant-assisted hierarchical lamellar MWW titanosilicate: a high-performance catalyst for selective oxidations involving bulky substrates. Catalysis Science and Technology, 2017, 7, 2874-2885.	4.1	28
132	The intrinsic properties of FA _(1â^'x) MA _x PbI ₃ perovskite single crystals. Journal of Materials Chemistry A, 2017, 5, 8537-8544.	10.3	152
133	Synthesis and Structure Determination of Largeâ€Pore Zeolite SCMâ€14. Chemistry - A European Journal, 2017, 23, 16829-16834.	3.3	24
134	Application of X-ray Diffraction and Electron Crystallography for Solving Complex Structure Problems. Accounts of Chemical Research, 2017, 50, 2737-2745.	15.6	69
135	Topotactic Reduction toward a Noncentrosymmetric Deficient Perovskite Tb _{0.50} Ca _{0.50} Mn _{0.96} O _{2.37} with Ordered Mn Vacancies and Piezoelectric Behavior. Chemistry of Materials, 2017, 29, 9840-9850.	6.7	7
136	Unusual Long-Range Ordering Incommensurate Structural Modulations in an Organic Molecular Ferroelectric. Journal of the American Chemical Society, 2017, 139, 15900-15906.	13.7	30
137	Stomata-like metal peptide coordination polymer. Journal of Materials Chemistry A, 2017, 5, 23440-23445.	10.3	9
138	A crystalline AlPO4-5 intermediate: designed synthesis, structure, and phase transformation. Dalton Transactions, 2017, 46, 12209-12216.	3.3	6
139	A Water Based Synthesis of Ultrathin Hydrated Vanadium Pentoxide Nanosheets for Lithium Battery Application: Free Standing Electrodes or Conventionally Casted Electrodes?. Electrochimica Acta, 2017, 252, 254-260.	5.2	14
140	Electrocatalysis: Hierarchical Co(OH)F Superstructure Built by Lowâ€Dimensional Substructures for Electrocatalytic Water Oxidation (Adv. Mater. 28/2017). Advanced Materials, 2017, 29, .	21.0	0
141	PKUâ€21: A Novel Layered Germanate Built from Ge ₇ and Ge ₁₀ Clusters for CO ₂ Separation. Chemistry - A European Journal, 2017, 23, 17879-17884.	3.3	0
142	Ultraquantum magnetoresistance in the Kramers-Weyl semimetal candidate βâ^'Ag2Se. Physical Review B, 2017, 96, .	3.2	27
143	Ultrafast epitaxial growth of metre-sized single-crystal graphene on industrial Cu foil. Science Bulletin, 2017, 62, 1074-1080.	9.0	454
144	Superconductivity of Perovskite Ba1â^'x Y x (Bi0.2Pb0.8)O3â~'δ. Journal of Superconductivity and Novel Magnetism, 2017, 30, 1705-1712.	1.8	10

#	Article	IF	CITATIONS
145	Zeolite A synthesized from alkaline assisted pre-activated halloysite for efficient heavy metal removal in polluted river water and industrial wastewater. Journal of Environmental Sciences, 2017, 56, 254-262.	6.1	91
146	Hierarchical Co(OH)F Superstructure Built by Lowâ€Ðimensional Substructures for Electrocatalytic Water Oxidation. Advanced Materials, 2017, 29, 1700286.	21.0	227
147	Rücktitelbild: Elucidation of Adsorbate Structures and Interactions on BrÃ,nsted Acid Sites in Hâ€ZSMâ€5 by Synchrotron Xâ€ray Powder Diffraction (Angew. Chem. 20/2016). Angewandte Chemie, 2016, 128, 6214-6214.	2.0	0
148	Multiferroicity Broken by Commensurate Magnetic Ordering in Terbium Orthomanganite. ChemPhysChem, 2016, 17, 1098-1103.	2.1	6
149	Undulated 2D Covalent Organic Frameworks Based on Bowlâ€Shaped Cyclotricatechylene. Chinese Journal of Chemistry, 2016, 34, 783-787.	4.9	13
150	Self‧upporting Metal–Organic Layers as Single‧ite Solid Catalysts. Angewandte Chemie - International Edition, 2016, 55, 4962-4966.	13.8	303
151	Adsorption Properties of MFM-400 and MFM-401 with CO ₂ and Hydrocarbons: Selectivity Derived from Directed Supramolecular Interactions. Inorganic Chemistry, 2016, 55, 7219-7228.	4.0	41
152	Innenrücktitelbild: Self-Supporting Metal-Organic Layers as Single-Site Solid Catalysts (Angew. Chem.) Tj ETQq	0	/Qverlock 10
153	Structure modulations in nonlinear optical (NLO) materials Cs2TB4O9(T= Ge, Si). Acta Crystallographica Section B: Structural Science, Crystal Engineering and Materials, 2016, 72, 194-200.	1.1	13
154	PKU-20: A new silicogermanate constructed from sti and asv layers. Microporous and Mesoporous Materials, 2016, 224, 384-391.	4.4	5
155	Accurate structure determination of a borosilicate zeolite EMM-26 with two-dimensional 10 × 10 ring channels using rotation electron diffraction. Inorganic Chemistry Frontiers, 2016, 3, 1444-1448.	6.0	27
156	A multi-dimensional quasi-zeolite with 12 × 10 × 7-ring channels demonstrates high thermal stability and good gas adsorption selectivity. Chemical Science, 2016, 7, 3025-3030.	7.4	12
157	Selective Adsorption of Sulfur Dioxide in a Robust Metal–Organic Framework Material. Advanced Materials, 2016, 28, 8705-8711.	21.0	214
158	Structure determination of modulated structures by powder X-ray diffraction and electron diffraction. Inorganic Chemistry Frontiers, 2016, 3, 1351-1362.	6.0	10
159	Recent Advances in the Synthesis and Application of Twoâ€Dimensional Zeolites. Advanced Energy Materials, 2016, 6, 1600441.	19.5	65
160	A one-step water based strategy for synthesizing hydrated vanadium pentoxide nanosheets from VO ₂ (B) as free-standing electrodes for lithium battery applications. Journal of Materials Chemistry A, 2016, 4, 17988-18001.	10.3	38
161	Pressure-Driven Cooperative Spin-Crossover, Large-Volume Collapse, and Semiconductor-to-Metal Transition in Manganese(II) Honeycomb Lattices. Journal of the American Chemical Society, 2016, 138, 15751-15757.	13.7	91
162	A Cuâ€Based Nanoparticulate Film as Superâ€Active and Robust Catalyst Surpasses Pt for Electrochemical H ₂ Production from Neutral and Weak Acidic Aqueous Solutions. Advanced Energy Materials, 2016, 6, 1502319.	19.5	36

#	Article	IF	CITATIONS
163	Elucidation of Adsorbate Structures and Interactions on BrÃ,nsted Acid Sites in Hâ€ZSMâ€5 by Synchrotron Xâ€ray Powder Diffraction. Angewandte Chemie - International Edition, 2016, 55, 5981-5984.	13.8	33
164	Self-Assembly of Cetyltrimethylammonium Bromide and Lamellar Zeolite Precursor for the Preparation of Hierarchical MWW Zeolite. Chemistry of Materials, 2016, 28, 4512-4521.	6.7	88
165	Selfâ€Supporting Metal–Organic Layers as Singleâ€Site Solid Catalysts. Angewandte Chemie, 2016, 128, 5046-5050.	2.0	61
166	Elucidation of Adsorbate Structures and Interactions on BrÃ,nsted Acid Sites in Hâ€ZSMâ€5 by Synchrotron Xâ€ray Powder Diffraction. Angewandte Chemie, 2016, 128, 6085-6088.	2.0	14
167	A ruthenium water oxidation catalyst based on a carboxamide ligand. Dalton Transactions, 2016, 45, 3272-3276.	3.3	21
168	Highly crystalline covalent organic frameworks from flexible building blocks. Chemical Communications, 2016, 52, 4706-4709.	4.1	83
169	Hydrothermal assembly of various dimensional pure-inorganic copper–molybdenum frameworks. CrystEngComm, 2016, 18, 521-524.	2.6	5
170	Pyrazolate-Based Porphyrinic Metal–Organic Framework with Extraordinary Base-Resistance. Journal of the American Chemical Society, 2016, 138, 914-919.	13.7	303
171	<mml:math xmlns:mml="http://www.w3.org/1998/Math/MathML"><mml:mrow><mml:mrow><mml:mo>(</mml:mo><mml:r Ion-exchange synthesis of large single-crystal and highly two-dimensional electron. Physical Review B, 2015. 92</mml:r </mml:mrow></mml:mrow></mml:math 	nsyb> <mr< td=""><td>nl:mi>Li</td></mr<>	nl:mi>Li
172	Immobilization of a Molecular Ruthenium Catalyst on Hematite Nanorod Arrays for Water Oxidation with Stable Photocurrent. ChemSusChem, 2015, 8, 3242-3247.	6.8	49
173	Monodisperse Sandwichâ€Like Coupled Quasiâ€Graphene Sheets Encapsulating Ni ₂ P Nanoparticles for Enhanced Lithiumâ€Ion Batteries. Chemistry - A European Journal, 2015, 21, 9229-9235.	3.3	50
174	Alkene Epoxidation Catalysts [Ru(pdc)(tpy)] and [Ru(pdc)(pybox)] Revisited: Revealing a Unique Ru ^{IV} â•O Structure from a Dimethyl Sulfoxide Coordinating Complex. ACS Catalysis, 2015, 5, 3966-3972.	11.2	10
175	PKU-3: An HCl-Inclusive Aluminoborate for Strecker Reaction Solved by Combining RED and PXRD. Journal of the American Chemical Society, 2015, 137, 7047-7050.	13.7	33
176	Approaching the structure of REBaB9O16 (RE = rare earth) by characterization of a new analogue Ba6Bi9B79O138. Journal of Materials Chemistry C, 2015, 3, 4431-4437.	5.5	12
177	Catalytic Water Oxidation by a Molecular Ruthenium Complex: Unexpected Generation of a Single-Site Water Oxidation Catalyst. Inorganic Chemistry, 2015, 54, 4611-4620.	4.0	37
178	Soluble Silver Acetylide for the Construction and Structural Conversion of All-Alkynyl-Stabilized High-Nuclearity Homoleptic Silver Clusters. Crystal Growth and Design, 2015, 15, 2505-2513.	3.0	22
179	A luminescent Zr-based metal–organic framework for sensing/capture of nitrobenzene and high-pressure separation of CH ₄ /C ₂ H ₆ . Journal of Materials Chemistry A, 2015, 3, 23493-23500.	10.3	22
180	Unusual Strong Incommensurate Modulation in a Tungsten-Bronze-Type Relaxor PbBiNb ₅ O ₁₅ . Journal of the American Chemical Society, 2015, 137, 13468-13471.	13.7	37

#	Article	IF	CITATIONS
181	A Crystalline Mesoporous Germanate with 48â€Ring Channels for CO ₂ Separation. Angewandte Chemie - International Edition, 2015, 54, 7290-7294.	13.8	26
182	Construct Polyoxometalate Frameworks through Covalent Bonds. Inorganic Chemistry, 2015, 54, 8699-8704.	4.0	15
183	An Iron-based Film for Highly Efficient Electrocatalytic Oxygen Evolution from Neutral Aqueous Solution. ACS Applied Materials & Interfaces, 2015, 7, 21852-21859.	8.0	161
184	Fine-Tuning of Crystal Packing and Charge Transport Properties of BDOPV Derivatives through Fluorine Substitution. Journal of the American Chemical Society, 2015, 137, 15947-15956.	13.7	224
185	A 3D 12â€Ring Zeolite with Ordered 4â€Ring Vacancies Occupied by (H ₂ O) ₂ Dimers. Chemistry - A European Journal, 2014, 20, 16097-16101.	3.3	17
186	Supra-molecular assembly of aromatic proton sponges to direct the crystallization of extra-large-pore zeotypes. Proceedings of the Royal Society A: Mathematical, Physical and Engineering Sciences, 2014, 470, 20140107.	2.1	7
187	Construction of Mesoporous Frameworks with Vanadoborate Clusters. Angewandte Chemie - International Edition, 2014, 53, 3608-3611.	13.8	46
188	SU-79: a novel germanate with 3D 10- and 11-ring channels templated by a square-planar nickel complex. Inorganic Chemistry Frontiers, 2014, 1, 278-283.	6.0	6
189	A Germanosilicate Structure with 11×11×12â€Ring Channels Solved by Electron Crystallography. Angewandte Chemie - International Edition, 2014, 53, 5868-5871.	13.8	69
190	Thermally/hydrolytically stable covalent organic frameworks from a rigid macrocyclic host. Chemical Communications, 2014, 50, 788-791.	4.1	67
191	Layered V–B–O polyoxometalate nets linked by diethylenetriamine complexes with dangling amine groups. Dalton Transactions, 2014, 43, 15283-15286.	3.3	13
192	EMM-23: A Stable High-Silica Multidimensional Zeolite with Extra-Large Trilobe-Shaped Channels. Journal of the American Chemical Society, 2014, 136, 13570-13573.	13.7	71
193	3D Open-Framework Vanadoborate as a Highly Effective Heterogeneous Pre-catalyst for the Oxidation of Alkylbenzenes. Chemistry of Materials, 2013, 25, 5031-5036.	6.7	61
194	Stepwise tuning of the substituent groups from mother BTB ligands to two hexaphenylbenzene based ligands for construction of diverse coordination polymers. CrystEngComm, 2013, 15, 8511.	2.6	9
195	A silicogermanate with 20-ring channels directed by a simple quaternary ammonium cation. Dalton Transactions, 2013, 42, 1360-1363.	3.3	27
196	Three-dimensional rotation electron diffraction: software <i>RED</i> for automated data collection and data processing. Journal of Applied Crystallography, 2013, 46, 1863-1873.	4.5	264
197	Irreversible Network Transformation in a Dynamic Porous Host Catalyzed by Sulfur Dioxide. Journal of the American Chemical Society, 2013, 135, 4954-4957.	13.7	123
198	Germanate with Three-Dimensional 12 × 12 × 11-Ring Channels Solved by X-ray Powder Diffraction with Charge-Flipping Algorithm. Inorganic Chemistry, 2013, 52, 10238-10244.	4.0	9

#	Article	IF	CITATIONS
199	Disorder in Extra-Large Pore Zeolite ITQ-33 Revealed by Single Crystal XRD. Crystal Growth and Design, 2013, 13, 4168-4171.	3.0	13
200	Synthesis of an extra-large molecular sieve using proton sponges as organic structure-directing agents. Proceedings of the National Academy of Sciences of the United States of America, 2013, 110, 3749-3754.	7.1	103
201	Rücktitelbild: A Tailor-Made Molecular Ruthenium Catalyst for the Oxidation of Water and Its Deactivation through Poisoning by Carbon Monoxide (Angew. Chem. 15/2013). Angewandte Chemie, 2013, 125, 4370-4370.	2.0	Ο
202	Structure determination of [3Fe2S] complex with complicated pseudo-merohedric twinning. Zeitschrift Für Kristallographie, 2012, 227, 221-226.	1.1	3
203	SU-75: a disordered Ge10 germanate with pcu topology. Dalton Transactions, 2012, 41, 12358.	3.3	6
204	A novel 1D independent metal–organic nanotube based on cyclotriveratrylene ligand. CrystEngComm, 2012, 14, 112-115.	2.6	31
205	Epitaxial growth of core–shell zeolite X–A composites. CrystEngComm, 2012, 14, 2204.	2.6	26
206	Three low-dimensional open-germanates based on the 44 net. CrystEngComm, 2012, 14, 5465.	2.6	9
207	SU-62: Synthesis and Structure Investigation of a Germanate with a Novel Three-Dimensional Net and Interconnected 10- and 14-Ring Channels. Crystal Growth and Design, 2012, 12, 369-375.	3.0	13
208	The Structure of a Complex Open-Framework Germanate Obtained by Combining Powder Charge-Flipping and Simulated Annealing. Crystal Growth and Design, 2012, 12, 4853-4860.	3.0	10
209	Mullite-derivative Bi2MnxAl7â^'xO14 (xâ^¼ 1): structure determination by powder X-ray diffraction from a multi-phase sample. Dalton Transactions, 2012, 41, 2884.	3.3	2
210	Selectivity and direct visualization of carbon dioxide and sulfur dioxide in a decorated porous host. Nature Chemistry, 2012, 4, 887-894.	13.6	466
211	Cyclotricatechylene based porous crystalline material: Synthesis and applications in gas storage. Journal of Materials Chemistry, 2012, 22, 5369.	6.7	128
212	Achiral Co atalyst Induced Switches in Catalytic Asymmetric Reactions on Racemic Mixtures (RRM): From Stereodivergent RRM to Stereoconvergent Deracemization by Combination of Hydrogen Bond Donating and Chiral Amine Catalysts. Advanced Synthesis and Catalysis, 2012, 354, 2865-2872.	4.3	15
213	Intergrown New Zeolite Beta Polymorphs with Interconnected 12-Ring Channels Solved by Combining Electron Crystallography and Single-Crystal X-ray Diffraction. Chemistry of Materials, 2012, 24, 3701-3706.	6.7	43
214	Structure and catalytic properties of the most complex intergrown zeolite ITQ-39 determined by electron crystallography. Nature Chemistry, 2012, 4, 188-194.	13.6	178
215	One‣tep Catalytic Enantioselective αâ€Quaternary 5â€Hydroxyproline Synthesis: An Asymmetric Entry to Highly Functionalized αâ€Quaternary Proline Derivatives. Advanced Synthesis and Catalysis, 2012, 354, 1156-1162.	4.3	16
216	One dimensional infinite water wires incorporated in isostructural organic crystalline supermolecules with zwitterionic channels. CrystEngComm, 2011, 13, 1287-1290.	2.6	9

#	Article	IF	CITATIONS
217	Two Open-Framework Germanates with Nickel Complexes Incorporated into the Framework. Inorganic Chemistry, 2011, 50, 9921-9923.	4.0	19
218	Investigation of the GeO2-1,6-Diaminohexane-Water-Pyridine-HF Phase Diagram Leading to the Discovery of Two Novel Layered Germanates with Extra-Large Rings. Inorganic Chemistry, 2011, 50, 201-207.	4.0	29
219	Synthesis of a [3Fe2S] Cluster with Low Redox Potential from [2Fe2S] Hydrogenase Models: Electrochemical and Photochemical Generation of Hydrogen. European Journal of Inorganic Chemistry, 2011, 2011, 1100-1105.	2.0	19
220	Microporous Aluminoborates with Large Channels: Structural and Catalytic Properties. Angewandte Chemie - International Edition, 2011, 50, 12555-12558.	13.8	67
221	A complicated quasicrystal approximant â^Š ₁₆ predicted by the strong-reflections approach. Acta Crystallographica Section B: Structural Science, 2010, 66, 17-26.	1.8	12
222	Structure determination of the zeolite IM-5 using electron crystallography. Zeitschrift Für Kristallographie, 2010, 225, 77-85.	1.1	38
223	BiMnFe2O6, a polysynthetically twinned hcp MO structure. Chemical Science, 2010, 1, 751.	7.4	13
224	Structure determination of zeolites and ordered mesoporous materials by electron crystallography. Dalton Transactions, 2010, 39, 8355.	3.3	14
225	Quantitative Electron Diffraction for Crystal Structure Determination. Materials Research Society Symposia Proceedings, 2009, 1184, 31.	0.1	0
226	The ITQ-37 mesoporous chiral zeolite. Nature, 2009, 458, 1154-1157.	27.8	526
227	A tri-continuous mesoporous material with a silica pore wall following a hexagonal minimal surface. Nature Chemistry, 2009, 1, 123-127.	13.6	131
228	Open-Framework Germanate Built from the Hexagonal Packing of Rigid Cylinders. Inorganic Chemistry, 2009, 48, 9962-9964.	4.0	25
229	Construction of 3-fold interpenetrated pcu organic frameworks from methanetetrabenzoic acid with zigzag bipyridines. CrystEngComm, 2009, 11, 2277.	2.6	13
230	Organic hydrogen-bonded interpenetrating diamondoid frameworks from modular self-assembly of methanetetrabenzoic acid with linkers. CrystEngComm, 2009, 11, 978.	2.6	97
231	Organocatalytic Highly Enantioselective Conjugate Addition of Aldehydes to Alkylidine Malonates. Advanced Synthesis and Catalysis, 2008, 350, 657-661.	4.3	52
232	A zeolite family with chiral and achiral structures built from the same building layer. Nature Materials, 2008, 7, 381-385.	27.5	205
233	Synthesis and Structure of Polymorph B of Zeolite Beta. Chemistry of Materials, 2008, 20, 3218-3223.	6.7	80
234	SU-22 and SU-23: Layered Germanates Built from 4-Coordinated Ge ₇ Clusters Exhibiting Structural Variations on the 4 ⁴ Topology. Crystal Growth and Design, 2008, 8, 3695-3699.	3.0	24

#	Article	IF	CITATIONS
235	Pd0.213Cd0.787 and Pd0.235Cd0.765 Structures: Their Longc Axis and Composite Crystals, Chemical Twinning, and Atomic Site Preferences. Chemistry - A European Journal, 2007, 13, 1394-1410.	3.3	34
236	Fourâ€Dimensional Space Groups for Pedestrians: Composite Structures. Chemistry - an Asian Journal, 2007, 2, 1204-1229.	3.3	23
237	New Barium Cobaltite Series Ban+1ConO3n+3(Co8O8):  Intergrowth Structure Containing Perovskite and CdI2-Type Layers. Inorganic Chemistry, 2006, 45, 9151-9153.	4.0	48
238	Crystal Growth and Structure Determination of Oxygen-Deficient Sr6Co5O15. Inorganic Chemistry, 2006, 45, 8394-8402.	4.0	34
239	Phase Equilibrium of the In2O3â^'TiO2â^'MO (M = Ca, Sr) Systems and the Structure of In6Ti6CaO22. Chemistry of Materials, 2005, 17, 2186-2192.	6.7	11
240	Volcanic relationship between wettability of the interface and water migration rate in solar steam generation systems. Nano Research, 0, , 1.	10.4	3
241	Design and Synthesis of a Zeolitic Organic Framework. Angewandte Chemie, 0, , .	2.0	ο